Pacific Northwest
NATIONAL LABORATORY

PNNL-38654

REBOUND: Reverse Engineering Bidirectional Outflow Under Non-Equilibrium Diffusion

October 2025

Stephen J. Young (co-PI)
Mavis Boamah-Agyemang (co-PI)
Ilya Amburg
Mark Bowden
Pravalika Butreddy
Yunxiang Chen
Sandilya Garimella
Trent Graham
Zuri Mao
Joshua Suetterlein
Chao Zeng

U.S. DEPARTMENT of ENERGY

Prepared for the U.S. Department of Energy
under Contract DE-AC05-76RL01830

DISCLAIMER

PACIFIC NORTHWEST NATIONAL LABORATORY
operated by
BATTELLE
for the
UNITED STATES DEPARTMENT OF ENERGY
under Contract DE-AC05-76RL01830

Printed in the United States of America

Available to DOE and DOE contractors from
the Office of Scientific and Technical Information,
P.O. Box 62, Oak Ridge, TN 37831-0062
www.osti.gov
ph: (865) 576-8401
fox: (865) 576-5728
email: reports@osti.gov

Available to the public from the National Technical Information Service
5301 Shawnee Rd., Alexandria, VA 22312
ph: (800) 553-NTIS (6847)
or (703) 605-6000
email: info@ntis.gov
Online ordering: http://www.ntis.gov

PNNL-38654

REBOUND: Reverse Engineering Bidirectional Outflow Under Non-Equilibrium Diffusion

October 2025

Stephen J. Young (co-PI)
Mavis Boamah-Agyemang (co-PI)
Ilya Amburg
Mark Bowden
Pravalika Butreddy
Yunxiang Chen
Sandilya Garimella
Trent Graham
Zuri Mao
Joshua Suetterlein
Chao Zeng

Prepared for
the U.S. Department of Energy
under Contract DE-AC05-76RL01830

Pacific Northwest National Laboratory
Richland, Washington 99354

Abstract

Rare-earth elements (REEs) are essential for electronics, renewable energy, and defense technologies. However, the current supply of REEs relies on mining concentrated in a few countries and energy-intensive separations. DOE's Basic Energy Sciences (BES) program has launched a grand challenge which aims to ensure a sustainable supply of critical REEs by developing innovative and environmentally friendly separation methods. As an alternative to costly and harmful traditional methods, the Non-Equilibrium Transport Driven Separations (NETS) initiative has created a microfluidic Y-channel co-flow method that applies external fields to exploit magneto- and electrohydrodynamic effects for separating dilute REE ions from complex feedstocks. Computational fluid dynamics (CFD) studies have identified a few operating conditions with promising ion selectivity and separation efficiency. However, challenges remain regarding Y-channel versatility across feedstocks and accurate incorporation of physical phenomena into CFD models. In this work, we develop a multi-fidelity modelling approach which integrates experimental results with CFD simulation to build a surrogate model for the dependence of separation efficiency to variation of design parameters. The surrogate model enables a reinforcement learning (RL) method to adaptively launch CFD and experimental runs, improving model fidelity around optimal Y-channel parameters.

Acknowledgments

This research was supported by the PCSD Mission Seed Investment, under the Laboratory Directed Research and Development (LDRD) Program at Pacific Northwest National Laboratory (PNNL). PNNL is a multi-program national laboratory operated for the U.S. Department of Energy (DOE) by Battelle Memorial Institute under Contract No. DE-AC05-76RL01830.

Acronyms and Abbreviations

REE: Rare Earth Elements

CFD: Computational Fluid Dynamics

LCM: Laminar Co-flow Method

SciMR: Scientific Map Reduce

Contents

Figures

Tables

1.0 Introduction

To ensure a reliable and sustainable supply of critical rare earth elements for advanced technologies and national security, the Department of Energy's Rare Earth Grand Challenge focuses on innovative, efficient, and environmentally friendly separation methods from unconventional sources. These elements, vital for renewable energy systems, electronics, and defense applications, are difficult to separate from complex and dilute feedstocks due to their similar chemical properties. Traditional separation methods use organic extractant ligands, which are costly and environmentally harmful.

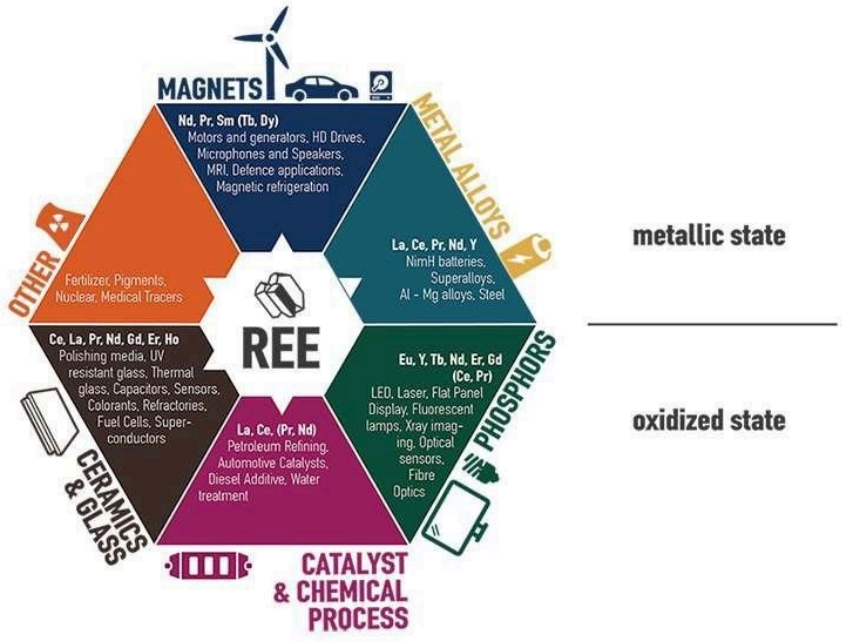

Figure 1: Applications of REE across a variety of modern technologies. Image developed by the CaptuREE project for the 2024 iGEM Jamboree

As an alternative to costly and harmful traditional methods, the Non-Equilibrium Transport Driven Separations (NETS) initiative has created the microfluidic laminar co-flow method, referred to as the Y-channel (see Figure). The Y-channel is designed to exploit electrohydrodynamic effects for the selective separation of trivalent, divalent, and monovalent cations from complex feedstocks. This microfluidic device capitalizes on the interplay between flow dynamics, electric fields, and diffusion. A pressure gradient drives horizontal flow, while an external electric field induces the vertical migration of ions, leveraging differences in their charge and mobility. Although magnetic separation is effective for certain REEs with strong magnetic susceptibilities, its applicability is limited due to the weak paramagnetic nature of some REE ions. In contrast, electric-field-based separation has emerged as a promising alternative for selectively isolating REEs from one another and competing non-REE ions. Computational Fluid Dynamics (CFD) studies have identified operational conditions which show significant potential for enhanced ion selectivity and separation efficiency. However, broader questions about the universal application of Y-channels across different complex feedstocks, as well as incorporating additional physical phenomena, such as reactions, nucleation, crystal growth, surface charge, transport, and electromobility of

ions and particles in solutions into the CFD models remain, necessitating further research to explore its versatility and scalability.

In order to potentially scale-up the laminar co-flow cells to industrial scale production of REEs it will be necessary to have a robust understanding of the separation performance across a variety of environmental and design conditions. In particular, this will require a deep understanding of the relationships between the design parameters of laminar co-flow cells (e.g., channel width, channel length, electric field strength, magnetic field strength, electric field location, REE source flow rate, precipitating agent, Y-split angle, etc.). Specifically, it desirable to identify conditions which optimize the preferential separation rate of the REE species of interest relative to costs. While it is theoretically possible to identify the optimum over the design space through brute-force exploration, the dimensionality of the design space and the necessity of for physical experimentation makes this approach impractical and expensive. Alternatively, brute force search can be used with the existing CFD models, however as high-fidelity models have significant computational costs this can also be expensive. Additionally, while providing insight into the dynamics within the Y-cell the accuracy of the existing CFD simulations is limited by not including all the relevant processes, including chemical reactions and precipitation of REEs in the laminar flow and on the cell boundaries. As a consequence, in order to, identify the optimal design parameters for separation it is necessary to develop methods which can explore a high-dimensional design space and integrate experimental and multi-fidelity data into a unified process.

To address this challenge, we provide a generalized framework which integrates simulation results from distributed computing resources and experimental results (potentially from a future automated laboratory) to build a surrogate model for the system of interest (in this case the laminar co-flow cell). Integrated into this system is a reinforcement learning and optimization framework which dynamically selects now experimental conditions to evaluate (and whether to use a computational or experimental model) which will improve the fidelity of the surrogate model and improve the estimation of the optimal design parameters.

2.0 Background

2.1 Dissolved REE Sources

The laminar co-flow setup relies on an initial input source which is enriched in the REEs of interest. One promising potential avenue for a such source is the produced water (PW) that results from fracking procedures frequently used to increase the production rates of natural gas wells. PW is naturally occurring, often hypersaline water from subterranean geologic formations brought to the surface during oil and gas extraction.

The Bakken Formation in North Dakota and Montana is often identified as one of the most promising sources of REEs in North American PW (Smith et al. 2024), with some studies citing concentrations as high as 2,000 ng/L. The Bakken is a major tight oil system where petroleum is extracted from low-permeability rock via hydraulic fracturing, producing a brine known to be geochemically complex. Due to these high reported values, Bakken was initially regarded as a model for a "best-case scenario" REE-rich PW feedstock.

This was reinforced by a study (Flynn et al. 2025) that detailed REE concentrations within solid cores sampled from the Bakken Formation. However, the extension of this finding to PW is less certain because a different study which analyzed 15 PW samples in the Bakken Formation concluded that concentrations of all REEs and platinum group metals were below their respective instrumental detection limits (Xiao 2021).

The contradictory Bakken data necessitates a refined methodology for site selection and analysis. The needed PW requires primary REE concentrations from analysis of PW (and not associated solids in core samples) and site-specific assessment of the PW matrix (background electrolytes).

Based on these criteria, the Powder River Basin in Wyoming was identified as a more suitable area. The recommended concentrations of the matrix (pH, Iron, Calcium, Magnesium, Potassium, Sodium, Chloride, Sulfate, Fluoride, Bicarbonate) from the work of (Nye 2018) are presented in Figure 2 as well as the REE concentrations (0.1-10 ng/L) in Figure 3.

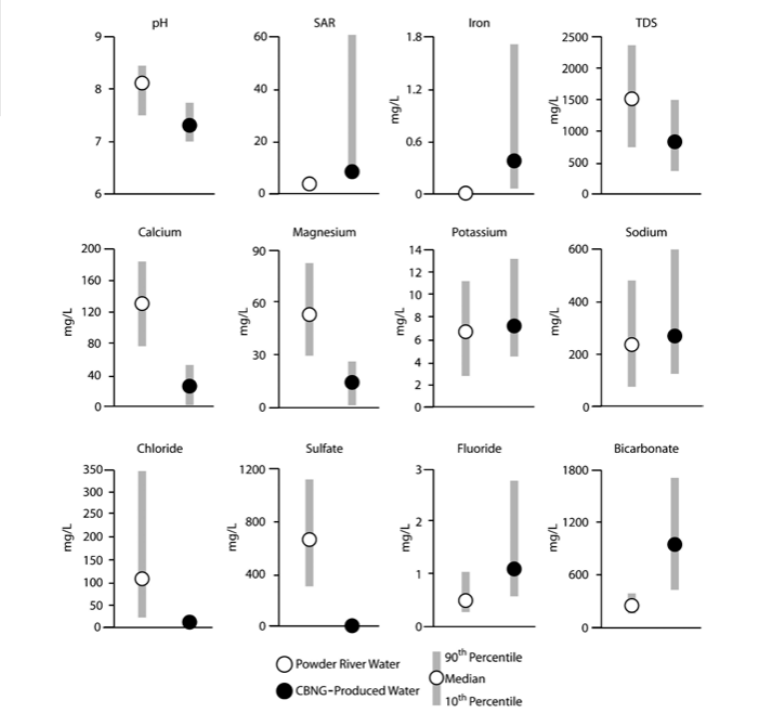

Figure 5. Major ion chemistry for the Powder River (open circles) and coalbed natural gas (CBNG)-produced water (closed circles). Circles represent the median value; gray rectangles represent the range between the 10th and 90th percentiles. Powder River data are from the U.S. Geological Survey and CBNG data are from Rice et al. (2002). TDS = total dissolved solid; SAR = sodium adsorption ratio.

Figure 2: Observed concentrations for non-REE ions dissolved in fracking waste. Image taken from (Nye 2018).

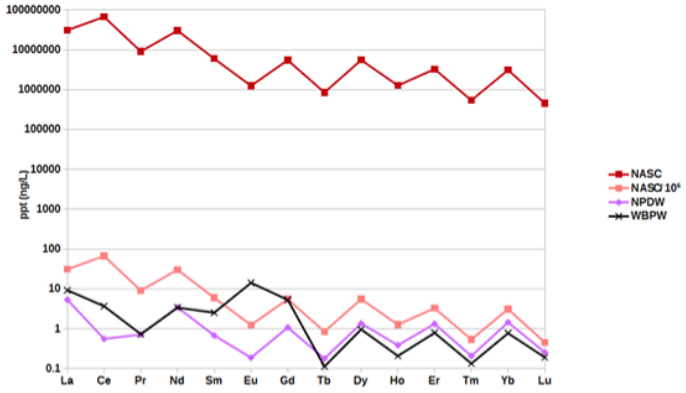

Figure 4: Chart of the absolute concentration in ppt of the North American Shale Composite (NASC in red), which has a pattern distinct from the North Pacific Deep Water (NPDW in purple). This can be seen by shifting NASC down by six orders of magnitude (pink). This difference in pattern is apparent in the Ce/Ce* concentrations, and also in the overall slope of the lines from LREEs to HREEs. We suggest a new normalization called Wyoming Basin Produced Waters (WBPW in black) which better matches on-shore basin groundwater. This normalization is distinct from both NASC and NPDW in Ce/Ce* behavior, and especially in MREE behavior. The HREEs are similar to the existing normalizations.

Figure 3: Concentration of dissolved REE ions in fracking waste. Figure taken from (Nye 2018)

Machine learning (ML) approaches are ideal for addressing the challenges identified to enhance REE separation accuracy and robustness across varying feedstocks, as it can process vast amounts of data to recognize complex patterns and relationships. Our high-level approach integrates CFD models, ML approximations, an optimizer, an automated laboratory, and a RL controller to ensure continuous data flow and optimization, see Figure 4. The REBOUND architecture can be thought of as having 4 primary components: 1) data generation, 2) surrogate modelling, 3) optimization, and 4) reinforcement learning. These four components of the

REBOUND workflow are orchestrated by runtime system which we developed called Scientific Map Reduce (SciMR). Because of the modular framework of SciMR, each of the four components can be readily swapped out for alternative approaches. We provide here a high-level summary of each of the four components, and defer detailed discussions to later in this section.

For REBOUND, the data generation component consists of three different sources: physical experiments with design parameters chosen to identify the boundaries of the feasible design space and two CFD simulations. One of these simulations is an extension of the work of [cite] and is implemented in COMSOL, a proprietary CFD simulation framework. The other CFD simulation uses the OpenFoam simulation framework, which is an open source alternative to COMSOL.

REBOUND uses an autoregressive GPR model as a surrogate model for the function from the design space to the separation performance. The choice of GPR for the surrogate model was motivated by the desire to incorporate uncertainties present in multi-fidelity data into downstream processes in the REBOUND architecture such as the RL controller and the optimization objective.

The REBOUND optimization and reinforcement learning is tightly coupled, yet extensible system that allows for the selection of a variety optimization frameworks, objective functions, and approaches to the reinforcement learning problem.

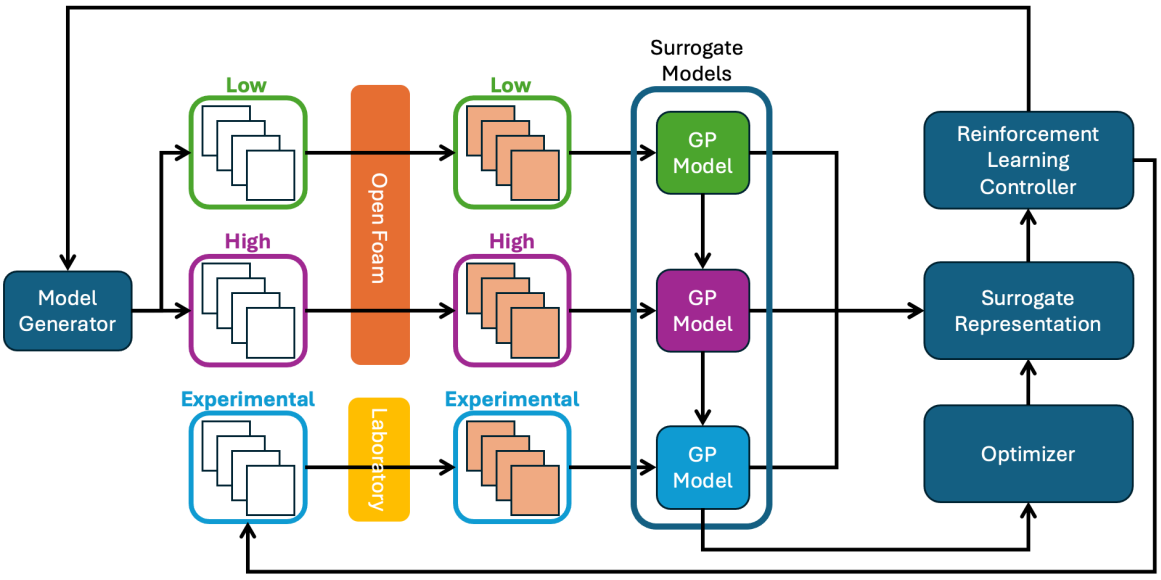

Figure 4: High-level schematic of the overall REBOUND architecture. The process integrates CFD models, ML approximations, an optimizer, an automated laboratory, and a reinforcement controller interwoven to ensure continuous data flow and optimization.

2.2 Laminar Co-Flow (Y-Cell) Experiments

To validate the results from the CFD simulations, initial experiments were conducted using a microfluidic double Y-channel functionalized with titanium sheets to generate an electric field, facilitating the separation of Dy^{3+} from simulated produced water containing nano-to- millimolar

concentrations of La^{3+}, Dy^{3+}, Mg^{3+}, Na^{+}, and Cl^{-} ions. REE solution mixtures were prepared, modeled after datasets obtained from the United States Geological Survey (USGS) to simulate produced water compositions accurately. This ensured that the study maintained environmental and industrial relevance while enhancing the precision of experimental consistency.

To design the laminar co-flow system for Rare Earth Element (REE) separation, a custom microfluidic cell was fabricated using polycarbonate sheets, a sandwiched parafilm membrane, and a titanium sheet (thickness 0.127mm) based on a previously reported method. (Qingpu et al. 2024) A parafilm sheet cut-out with a double-Y design is sandwiched between two polycarbonate sheet cutouts (thickness 1.6mm) and meticulously assembled with metallic screw fittings (diameter 3mm) to ensure structural integrity. Barb fittings were glued onto the strategically placed holes (inner diameter 1.6mm) to serve as inlet and outlet connections for solution flow. The microfluidic cells were constructed with precise specifications (see Figure 5: Schematic of Laminar Co-Flow Cell) tailored to optimize REE separation processes. Additionally, a chlordized Ag/AgCl wire electrode (reference electrode) was placed into one of the outlet solutions, and a potentiostat was used for varying voltages across the Y-channel.

For magnetic field experiments, a 1T magnet bar was placed right beside the LCM cell, closer to outlet 1 and inlet 1, as shown in Figure 8. Herein, the millimolar metal ions mixture came in through inlet 1, whereas the precipitating agent was flown through inlet 2. The quantification of REE separation efficiency was performed using Inductively Coupled Plasma Mass Spectrometry (ICP-MS) analysis. Output solutions from the system were analyzed to validate the effectiveness of the separation process and measure the yield of REEs, establishing a robust method for further studies and optimization in REE extraction processes.

Previous CFD simulations did not account for ion adsorption onto the Y-channel walls, as the role of the electrical double layer (EDL) phenomenon has yet to be fully quantified. To estimate the role of EDL in the separation process, we conducted an experiment designed to minimize the adsorption of charged analytes onto the Y-channel. To achieve this, we utilized a surface deactivation methods that included coating the channel walls with a thin layer of non-crosslinked polyacrylamide and flowing polysorbate 20 through the LCM cell before performing electric-field experiments. Ongoing experimental efforts in NETS aim to effectively quantify the role of EDL in REE separations, and our proposed CFD simulations can leverage from these previous findings garnered by NETS.

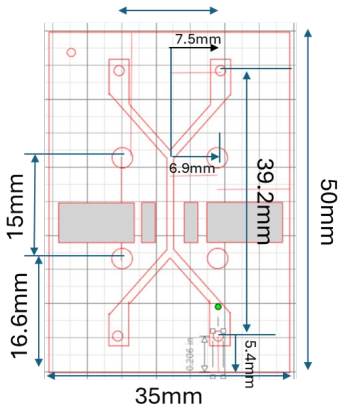

Figure 5: Schematic of Laminar Co-Flow Cell

Figure 6: Example of laminar co-flow cell used for experiments using electric field.

Figure 7: Experimental arrangement with an electric field laminar co-flow cell and a pumping setup for water flow.

Table 1 Composition of REE mixtures utilized in electric field experiments

Input REE Mixtures	La (nM)	Dy (nM)	Mg (nM)	Na (nM)	La (ppb)	Dy (ppb)	Mg (ppb)	Na (ppb)
solution A	50	25	50	500	6.95	4.05	1.215	11.495
Solution B	10	5	50	500	1.39	0.8	1.215	11.495
Solution C	100	50	50	500	13.9	8.1	1.215	11.495

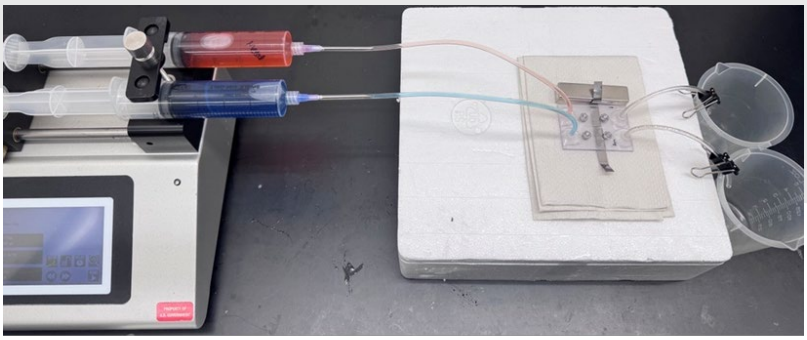

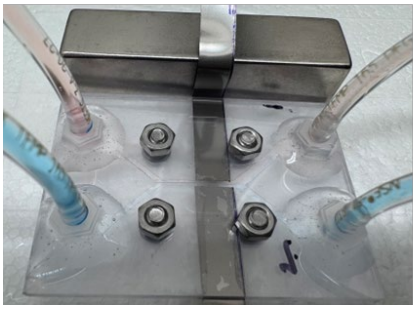

Ions	Concentration (mM)
La^{3+}	5
Dy^{3+}	2.5
Mg^{2+}	250
Na^{+}	500

Figure 8 Experimental arrangement with externally applied magnetic field (with 1T bar magnet) to the laminar co-flow cell and pumping setup for the solutions flowing at 4 mL/hour. The feedstock metal (input mixture - see side table for its composition) solution is colored red, and the precipitating agent, 25 mM sodium oxalate, is colored blue.

2.3 CFD Models

In order to determine the Y-channel design parameters, such as inlet size, flow rate, electric/magnetic field strength, and outlet configurations which maximize yield from different feedstocks it is necessary to consider the effect of a variety of physical phenomena such as reactions, nucleation, crystal growth, surface charge, transport, and electromobility of ions and particles in solutions. To this end, selected phenomena are incorporated into a CFD simulation of the flow of the feedstock the Y-channel. The dynamic flow of feedstock passing through the Y-channel is simulated by solving the incompressible Navier-Stokes equation, and transport of ionic species is modeled using the Nernst-Planck equations, accounting for diffusion, convection, and electric field-driven migration. To accurately represent the influence of electrostatic interactions on ion distribution and mobility, the model incorporates the electrical double layer (EDL) using a modified Poisson–Nernst–Planck (PNP) framework, which captures potential gradients and ion accumulation near charged surfaces. Surface charge boundary conditions are implemented to dynamically couple local field strength with ion adsorption and reaction rates. Additionally, nucleation and crystal growth kinetics are incorporated via user-defined source terms in the mass transport equations, allowing for spatially resolved prediction of solid-phase formation. This multi-physics approach enables a predictive analysis of how variations in inlet velocity, electric or magnetic field strength, and outlet configuration influence separation performance and yield across a range of feedstock conditions. The multi-physics coupled CFD model is solved in the commercial Multiphysics COMSOL software and the OpenFoam open-source software.

COMSOL is a commercial solution for Computational Fluid Dynamics (CFD) simulations, offering a significant advantage in both time efficiency and accuracy over many open-source tools—our tests showed a 5x improvement in runtime with enhanced accuracy for our specific problem. However, deploying COMSOL on our cluster presented challenges due to the prohibitive costs associated with additional licensing options for direct cluster integration. To overcome these limitations, we developed a containerized solution that enabled the effective execution of COMSOL simulations in a cluster environment without requiring user interaction.

COMSOL supports the distribution of single binaries as standalone applications, which automatically install required runtime components and execute simulations upon launch. While this simplifies deployment in standalone environments, there are challenges when adapting the solution for clusters. A dialog box is displayed during execution, demanding user input initially, which is unsuitable for automated workflows. To tackle this, we containerized the application using Docker, employing a three-step process. First, we set up a graphical interface environment required for the initial installation of COMSOL's standalone binary. This step allows the GUI-based installation to complete successfully inside the container. Second, we created a new container stripped of the GUI setup but equipped with libraries that emulate a graphical environment. This adjustment ensures that simulations can run within the container without requiring user interaction with the display window. Finally, we configured automation scripts to terminate the application once the desired outputs are generated, discarding the display window that the simulation renders during execution.

Our containerized workflow was thoroughly tested within Docker and successfully run in the controlled environment. For deployment in a cluster setting, however, an additional step was required: porting the Docker container to Singularity, as our clusters do not support Docker directly. While this process is typically straightforward due to Singularity's compatibility with Docker images, debugging issues during the conversion consumed significant time and resources. The containerization workflow provided a prototype that worked successfully in Docker, and efforts are ongoing to finalize its migration to singularity for use in the cluster environment.

To perform the optimization of the separation process, the CFD simulations are linked to the optimization and acquisition process through the SciMR workflow orchestrator. The RL framework operates on the current surrogate model and provides candidate design parameters for further CFD simulations. These operating parameters are tested via the COMSOL and OpenFoam simulations and the results are used to update the surrogate model.
This loop continues until convergence is achieved. To enable this loop, the COMSOL and OpenFoam models are converted into an executable files which can be run from within the SciMR framework with arbitrary suggested operating parameters.

2.4 Surrogate Model

Since this single output case is what we are interested in, we focus on Gaussian Process Regression for functions of the form $f: R^n \to R$. In this case, the fundamental assumption is that the distribution (with uncertainty) of a $\big(f(x_1), \dots, f(x_k)\big)$ should be given by a multivariate Gaussian (normal) distribution $\mathcal{N}(\mu, \Sigma)$. The regression process relies on three parameters, $\mu: R^n \to R$ a prior estimate of the value of the function, $\sigma \in R^+$ a smoothing parameter, and $K: R^n \times R^n \to R$ a positive semi-definite kernel function which parametrizes the distance between of pairs of points. Given these regression parameters and a collection of known points $\{ (x\_i, f(x\_i))\}$ the distribution for a collection of sample points $(s\_1, \dots, s\_k)$ is given by

$$f(\mathrm{s}) \sim \mathcal{N}\left(\mu(\mathrm{s}) + \mathrm{K}(\mathrm{s},\mathrm{x})(\mathrm{K}(\mathrm{x},\mathrm{x}) + \sigma\mathrm{I})^{-1}\big(\mathrm{f}(\mathrm{x}) - \mu(\mathrm{x})\big), \mathrm{K}(\mathrm{s},\mathrm{s}) - \mathrm{K}(\mathrm{s},\mathrm{x})(\mathrm{K}(\mathrm{x},\mathrm{x}) + \sigma\mathrm{I})^{-1}\mathrm{K}(\mathrm{x},\mathrm{s})\right)$$

In essence, this means that the kernel function and σ control how uncertainty increases as we move away from known points and the evaluation points $f(x_i)$ serve to moderate our initial guess for the function value μ. In order to distinguish notationally between the observed function values and the distribution of potential values given by the Gaussian Process Regression, we will we use F to denote the associated collection of random variables.

In the context of REBOUND, we will maintain multiple different Gaussian Process Regression models for each level of fidelity -- for now, we discuss only a low-fidelity CFD simulation (F_L), a high-fidelity CFD simulation F_H, and experimental model F_E as it is straightforward to extend our approach to additional fidelities. Each model will have an independent smoothing parameter $(\sigma_L, \sigma_H, \sigma_E)$ which will be tuned based on our understanding of the uncertainties present in the model and the kernel function K will be the same for all three models (since it is a representation of the underlying structure of the parameter space). In order to couple the three models, we will define $\mu_L = 0$ (which is a standard zero-information prior), $\mu_H = E[F_L]$, and $\mu_E = E[F_H]$. That is, we assume that the mean behavior is well approximated by the mean behavior at the lower fidelity. It is worth noting that this function is well-defined (given a set of prior observed data). For example, considering

$$E[F_H(s)] = E[F_L(s)] + K(s,x)(K(x,x) + \sigma_H I)^{-1}(f(x) - E[F_L(x)])$$

we note that $(K(x,x) + \sigma_H)^{-1}(f(x) - \boldsymbol{E}[F_L(x)])$ is independent of the points of interest s, so can be thought of as a fixed vector conditioned on the prior observations. Noting that the i[th] row of $K(s,x)$ depends only on s_i we have that $E[F_H(s)]^T e_i$ can be calculated entirely in terms of s_i and the prior observations x.

3.0 Results and Products

3.1 Laminar Co-Flow Experiments

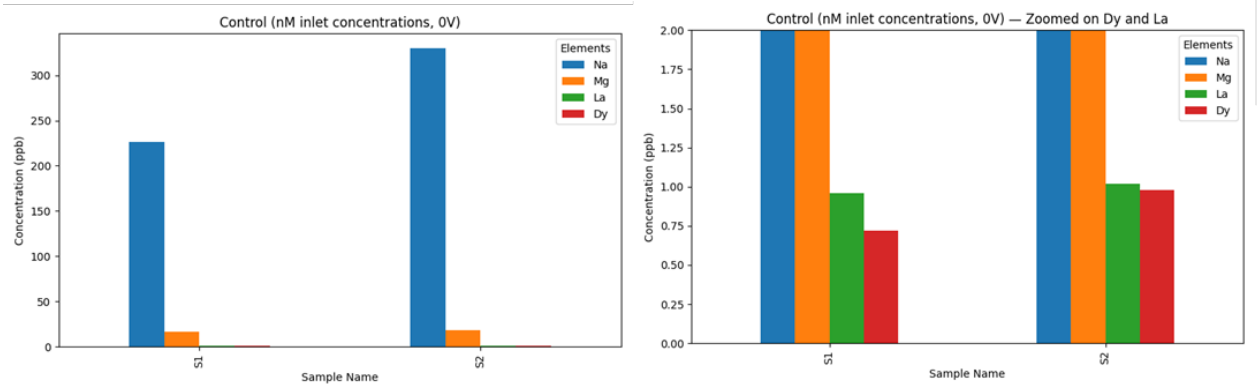

Figure 9 Results from control experiments for electric field measurements obtained at 0V externally applied using feedstock solution C. Right graph is a zoom-in version of the left graph.

Prior to conducting the main electric field experiments, we performed control measurements at 0V applied, flowing solutions at 4 mL/hour. ICP-MS results revealed a slight enrichment of Dy in outlet 2 under zero-voltage conditions, whereas roughly amount of La was collected from both outlets.

During electric field-driven separation runs, introducing solution C (see Table 1 Composition of REE mixtures utilized in electric field experiments) as the input mixture and applying 1V externally to the Ti plates resulted in approximately 1.5x enrichment of both dysprosium (Dy) and lanthanum (La) in outlet 1. Interestingly, varying the flow rate (2 to 4 mL/hour) and adjusting the applied voltage (1V, 4V, and 8V) had no measurable impact on the enrichment factor. This consistent behavior indicates that the separation process is predominantly governed by the inherent properties of the input solution rather than external operational conditions.

Furthermore, recycling the enriched solution from outlet 1 proved to be an effective strategy for improving separation efficiency. Iterative processing enabled a 2x enrichment of Dy and La in outlet 1, demonstrating the recycling approach's potential for maximizing rare earth element (REE) recovery. These findings emphasize the adaptability of the system and its suitability for future optimization, paving the way for more sustainable REE separation methodologies.

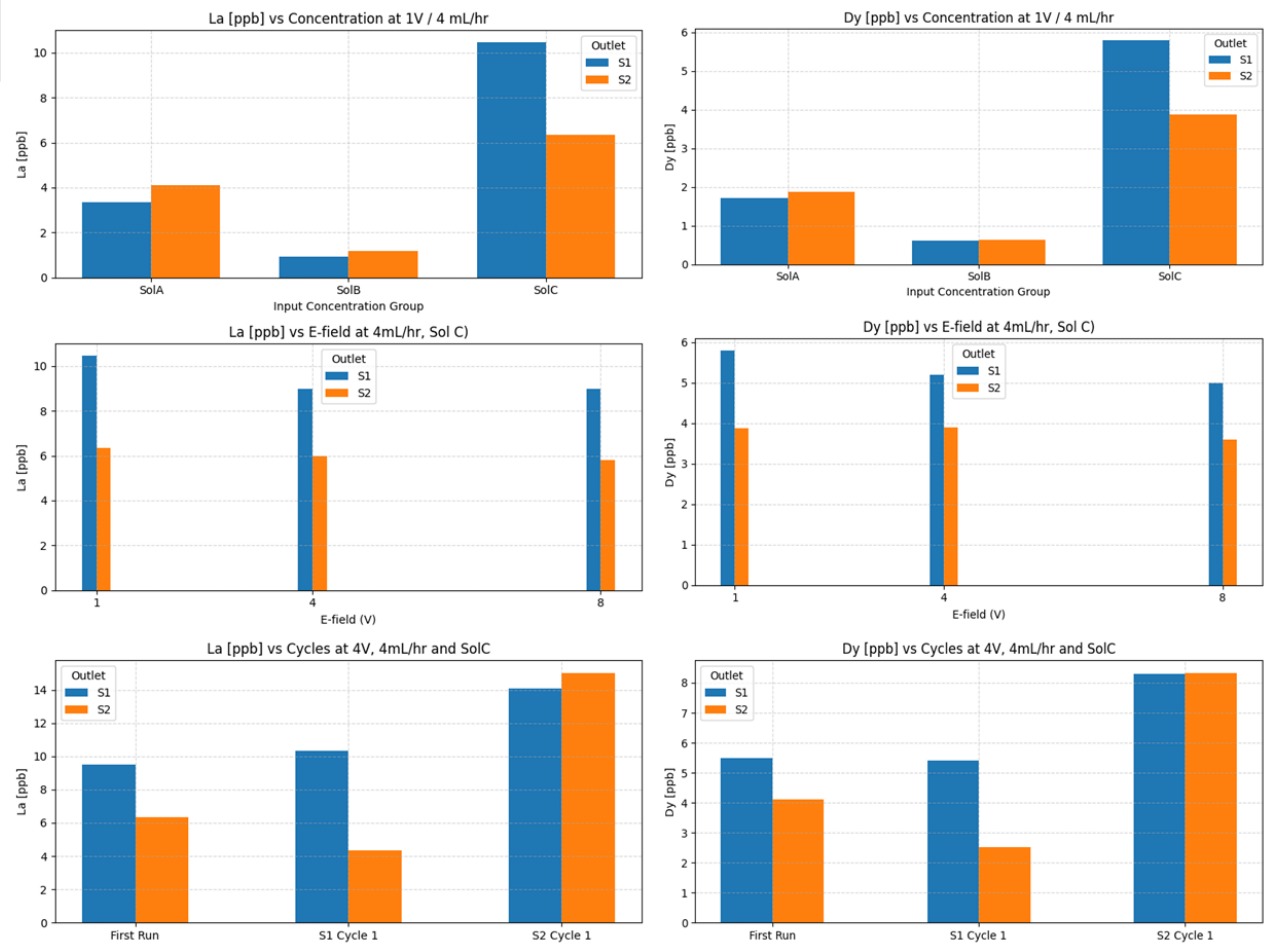

Figure 10 Results for E field experiments (Top row 1) with solutions mixtures A, B, and C at 4 mL/hour and 1V externally applied; (Middle row 2) with solution C at 1V, 4V, and 8V; and (Bottom row 3) recycling of outlet solutions obtained from initially flowing solution C at 4 mL/hour and 4V externally applied.

Results from Magnetic field-driven separation experiments: Our experiments demonstrated that precipitates collected from outlet 1 are enriched in dysprosium, while those from outlet 2 are enriched in lanthanum. This result aligns with expectations, as the 1T bar magnet is positioned closer to outlet 1. Dysprosium, being strongly paramagnetic, is more likely to respond to the magnetic field and move closer to the magnet after reacting with the precipitating agent, whereas lanthanum, which is weakly paramagnetic, remains less affected. To confirm that the dysprosium ions indeed moved in response to the magnetic field, we conducted co-flow experiments with colored solutions, as illustrated in Figure 8. The distinct lack of mixing observed between the colored solutions during these experiments confirms that it is the dysprosium ions, not the bulk solution, that respond to the magnetic field and migrate accordingly.

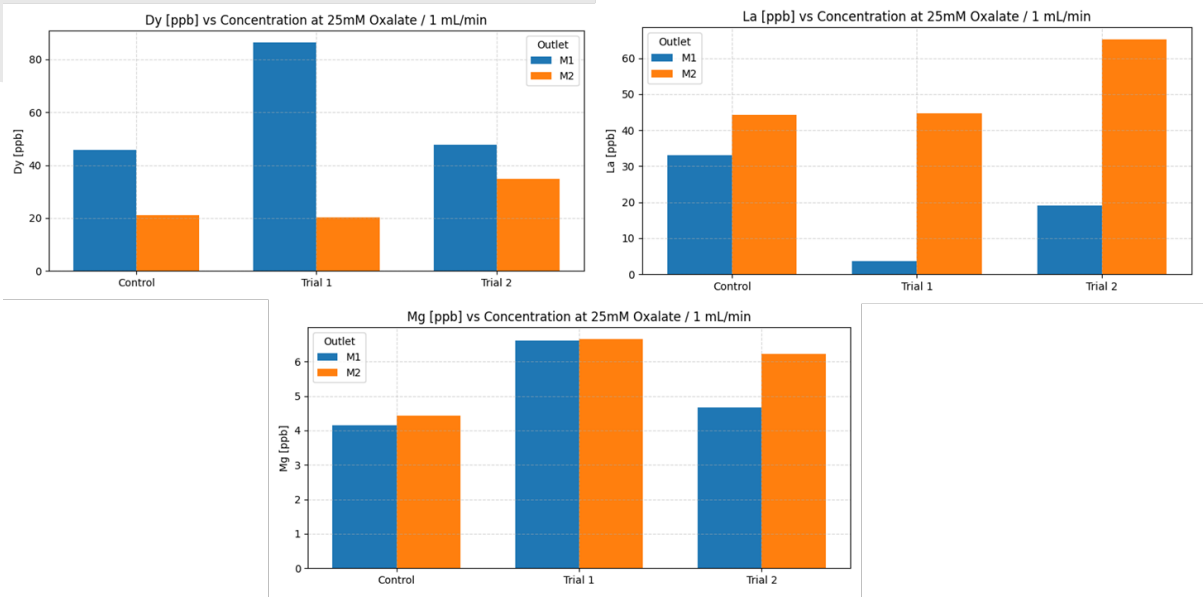

Figure 11 Results from magnetic field experiments with no colored solutions. Precipitate = ppt. M1 and M2 are precipitates from outlets 1 and 2, respectively.

Table 2 Results from magnetic field experiments with colored solutions. Precipitate = ppt. S1 and S2 are outlets 1 and 2, respectively.

	Na (ppm)	Mg (ppm)	La (ppm)	Dy (ppm)
S1 ppt concentrate	18.29	0.10	0.95	1.14
S2 ppt concentrate	16.76	0.51	2.08	0.39

Results from Electrical Double Layer (EDL) Suppression Experiments:
The initial attempt to suppress EDL effects using a polyacrylamide coating was unsuccessful, as the coating introduced gaps in the LCM cell, causing solution leakage during pumping and flow (see Figure 12 The Y-cell plates were coated with polyacrylamide using a spin coater (see left image). The assembled cell leaks due to potential channel blockage by the polyacrylamide coat (see right image). below). To address this issue, we adopted an alternative approach by flowing polysorbate 20 through the LCM cell prior to conducting the main E-field experiment. This adjustment ensured system integrity and allowed us to proceed with the investigations effectively. However, the ICP-MS results (see Table 3 below) for the outlet solutions obtained after suppressing EDL formation using polysorbate 20 are inconsistent, showing unexpectedly higher concentrations of both Dy and La in the outlet solutions compared to the inlet solutions.

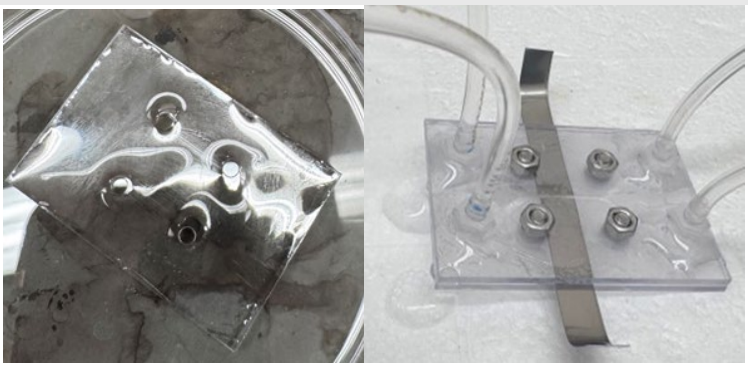

Figure 12 The Y-cell plates were coated with polyacrylamide using a spin coater (see left image). The assembled cell leaks due to potential channel blockage by the polyacrylamide coat (see right image).

Table 3 ICP-MS results from using a non-ionic surfactant: polysorbate 20 to suppress EDL formation. 0.1% Tween (polysorbate 20 – poly) solution was flowed through the double Y cell, followed by DI water rinse and Solution C run at 4mL/hour and 1V. S1 and S2 are outlets 1 and 2, respectively.

	Na (ppb)	Mg (ppb)	La (ppb)	Dy (ppb)
S1	85	2	67	11
S2	105	2	78	19

3.2 Scientific Map Reduce (SciMR)

SciMR (Scientific MapReduce) is a simplified framework designed to empower scientists by enabling them to scale applications from single-node execution to distributed processing across clusters. The purpose of SciMR is to provide an intuitive solution for running simulations or computations on multiple nodes in parallel while efficiently reducing the resulting data. Integrated directly with SLURM, the job management system widely employed in research environments, SciMR leverages its capabilities to streamline distributed task execution. This tool is lightweight and is implemented in Python to offer flexibility, yet it maintains the ability to launch jobs directly via the Linux command line, ensuring compatibility with traditional computational workflows.

SciMR employs a straightforward API that requires users to create only one class with three essential functions—making the framework accessible to individuals with varying levels of programming expertise. The first function, Init, launches initial jobs, enabling the parallel execution of computational tasks. The framework also provides two callback methods: one for processing individual job results, and another for handling job outputs alongside associated metadata. These callbacks give users the capability to refine, reduce, and aggregate computational results as needed, while also enabling the dynamic launching of new jobs based on intermediate findings. By scaling seamlessly from single-node execution to SLURM's

computational cluster, SciMR provides a robust testing environment for research workflows, facilitating the transition to large-scale computing.

Unlike larger frameworks such as Dask, which integrate deeply with the Python ecosystem and require extensive reliance on libraries like NumPy, SciMR remains lightweight and purpose-built for scientific computing contexts. While Dask is ideal for more complex workflows, SciMR is tailored for researchers seeking simplicity and direct command-line integration. Within the broader project, SciMR serves a pivotal role by enabling the efficient execution of simulations as the "mappers" and leveraging machine learning models during the "reduction" phase. This versatility underscores SciMR's value in managing distributed computational tasks for scientists aiming to scale their work efficiently and systematically.

4.0 References

Flynn, Jessica, Holly Shoulak, and Omid Ardakani. 2025. *A Preliminary Investigation into Rare Earth Element (REE) Distribution in the Organic-Rich Bakken Formation, Southeastern Saskatchewan*.

Nye, Charles, Davin Bagdonas, and Scott Quillinan. 2018 “A New Wyoming Basin Produced Waters REE Normalization and Its Application.” *Proceedings of the 43rd Workshop on Geothermal Reservoir Engineering*.

Smith, Kathryn H., Justin E. Mackey, Madison Wenzlick, Burt Thomas, and Nicholas S. Siefert. 2024. “Critical Mineral Source Potential from Oil & Gas Produced Waters in the United States.” *Science of The Total Environment* 929 (June): 172573. https://doi.org/10.1016/j.scitotenv.2024.172573.

Xiao, Feng. 2021. “Characterization and Treatment of Bakken Oilfield Produced Water as a Potential Source of Value-Added Elements.” *Science of The Total Environment* 770 (May): 145283. https://doi.org/10.1016/j.scitotenv.2021.145283.

Chen, Ziying, Zhan Li, Jia Chen, Parashuram Kallem, Fawzi Banat, and Hongdeng Qiu. "Recent Advances in Selective Separation Technologies of Rare Earth Elements: A Review." *Journal of Environmental Chemical Engineering* 10, no. 1 (2022/0/01/ 2022): 107104. https://doi.org/https://doi.org/10.1016/j.jece.2021.107104. https://www.sciencedirect.com/science/article/pii/S2213343721020819.

Higgins, Robert F, Thibault Cheisson, Bren E Cole, Brian C Manor, Patrick J Carroll, and Eric J Schelter. "Magnetic Field Directed Rare-Earth Separations." *Angewandte Chemie* 132, no. 5 (2020): 1867-72.

Hjertén, Stellan, and Bo-Liang Wu. "Studies of Fish Zona Pellucida by High-Performance Ion-Exchange Chromatography on Agarose Columns and Free Zone Electrophoresis." *Journal of Chromatography B: Biomedical Sciences and Applications* 341 (1985/01/01/ 1985): 295-304. https://doi.org/https://doi.org/10.1016/S0378-4347(00)84043-8. https://www.sciencedirect.com/science/article/pii/S0378434700840438.

Kumar, Amit, Han Geng, and Eric J. Schelter. "Harnessing Magnetic Fields for Rare-Earth Complex Crystallization–Separations in Aqueous Solutions." 10.1039/D2RA04729B. *RSC Advances* 12, no. 43 (2022): 27895-98. https://doi.org/10.1039/D2RA04729B. http://dx.doi.org/10.1039/D2RA04729B.

Mao, Zirui; Xu, Zhijie; Huang, Yang; Ricchiuti, Giovanna; Palmer, Bruce; Simonnin, Pauline G; Murugesan, Vijaykumar; Johnson, Grant E; Chun, Jaehun; Prabhakaran, Venkateshkumar. Harnessing Electric Fields for Rare Earth Element Recovery: A Computational Study of Electromigration and Flow Dynamics Using Dilute Feedstock. 12 March 2025 2025. ChemRxiv.

Sciences, National Academies of, Medicine, Division on Earth, Life Studies, Board on Chemical Sciences, and Committee on a Research Agenda for a New Era in Separation Science. "A Research Agenda for Transforming Separation Science." (2019).

Traore, Mory, Aijun Gong, Yiwen Wang, Lina Qiu, Yuzhen Bai, Weiyu Zhao, Yang Liu*, et al.* "Research Progress of Rare Earth Separation Methods and Technologies." *Journal of Rare Earths* 41, no. 2 (2023/02/01/ 2023): 182-89. https://doi.org/https://doi.org/10.1016/j.jre.2022.04.009. https://www.sciencedirect.com/science/article/pii/S1002072122001065.

Wang, Qingpu, Jaehun Chun, and Chinmayee V. Subban. "Influence of Concentration Gradients on Electroconvection at a Cation-Exchange Membrane Surface." *Langmuir* 40, no. 3 (2024/01/23 2024): 1613-22. https://doi.org/10.1021/acs.langmuir.3c02453. https://doi.org/10.1021/acs.langmuir.3c02453.

Wang, Qingpu, Yucheng Fu, Erin A. Miller, Duo Song, Philip J. Brahana, Andrew Ritchhart, Zhijie Xu*, et al.* "Selective Recovery of Critical Minerals from Simulated Electronic Wastes Via Reaction-Diffusion Coupling." *ChemSusChem* n/a, no. n/a: e202402372. https://doi.org/https://doi.org/10.1002/cssc.202402372. https://chemistry-europe.onlinelibrary.wiley.com/doi/abs/10.1002/cssc.202402372.

Wang, Qingpu, Elias Nakouzi, Elisabeth A. Ryan, and Chinmayee V. Subban. "Flow-Assisted Selective Mineral Extraction from Seawater." *Environmental Science & Technology Letters* 9, no. 7 (2022/07/12 2022): 645-49. https://doi.org/10.1021/acs.estlett.2c00229. https://doi.org/10.1021/acs.estlett.2c00229.

Wang, Qingpu, and Chinmayee V. Subban. "Flow-Driven Enhancement of Neodymium and Dysprosium Separation from Aqueous Solutions." 10.1039/D3SU00403A. *RSC Sustainability* 2, no. 5 (2024): 1400-07. https://doi.org/10.1039/D3SU00403A. http://dx.doi.org/10.1039/D3SU00403A.

PNNL-38654

Pacific Northwest National Laboratory

902 Battelle Boulevard
P.O. Box 999
Richland, WA 99354

1-888-375-PNNL (7665)

www.pnnl.gov